THE ETA CARINAE NEBULA AND CENTAURUS A NEAR 1400 Mc/s

I. OBSERVATIONS

By J. V. Hindman* and C. M. Wade*

[*Manuscript received May 27, 1959*]

Summary

Observations of two strong southern radio sources, the Eta Carinae Nebula (NGC 3372) and Centaurus A (13S4A), at a frequency near 1400 Mc/s, are described. The observations were made with a 36 ft transit-mounted paraboloidal aerial and a 21 cm hydrogen-line receiver modified for the reception of continuum radiation.

The flux density of the Eta Carinae Nebula near 1400 Mc/s is $5\cdot 82\times 10^{-24}$ W m^{-2} (c/s)$^{-1}$, with an estimated uncertainty of less than ± 20 per cent. This source appears to be fairly symmetrical, with a strong central condensation.

The flux density of Centaurus A is $1\cdot 3\times 10^{-23}$ W m^{-2} (c/s)$^{-1}$, with an estimated uncertainty of ± 20 per cent. The great angular extent of the object previously found at metre wavelengths is confirmed; at 1400 Mc/s the source covers 7° in declination and about 3° in Right Ascension. The central source associated with NGC 5128 is responsible for about 23 per cent. of the total flux, with the remainder arising in the extended part of the source. There is a well-marked secondary maximum in the extended component at $\alpha_{1950}\approx 13^{\mathrm{h}}\ 21^{\mathrm{m}}$, $\delta_{1950}\approx -44^{\circ}\cdot 7$.

I. Introduction

(*a*) *The Eta Carinae Nebula*

One of the most prominent galactic emission nebulae is NGC 3372, commonly known as the " Eta Carinae Nebula ". Photographs taken in Hα light show that it consists of a bright core less than half a degree in diameter, crossed by several absorption lanes, with fainter outer extensions which increase its overall angular diameter to 2° (Gum 1955). According to Bok, Bester, and Wade (1955), there may be a very faint Hα emission field underlying the nebula and extending for several degrees; this feature is probably unrelated to NGC 3372. Recently Mills, Little, and Sheridan (1956) have shown that the object is a strong emitter of radio waves at $85\cdot 5$ Mc/s.

Despite the prominence of NGC 3372, very little is known about its physical properties—temperature, density, mass, excitation, etc. Aside from an early study by Bok (1932), who found a density of 60 ions cm^{-3} for the inner regions of the nebula, the published data are almost entirely of a descriptive nature (Bailey 1908; Cederblad 1946; Gum 1955). The observations described in the present paper were undertaken to provide data for a determination of the general physical properties of the object; these will be discussed in the second paper of this series (Wade 1959). A secondary reason for the observational programme was that NGC 3372 is the only important galactic emission nebula too far south to be included in Westerhout's (1958) comprehensive survey at 1400 Mc/s.

* Division of Radiophysics, C.S.I.R.O., University Grounds, Chippendale, N.S.W.

(b) *Centaurus A*

The strong southern radio source Centaurus A (13S4A) was one of the first to be identified with an optically observable object. Bolton, Stanley, and Slee (1949) suggested that it is associated with the peculiar galaxy NGC 5128. This identification still appears to be correct. NGC 5128 is an anomalous object, appearing to be a spheroidal galaxy of Hubble type E_0 crossed by a dark band of obscuration. The radio-frequency counterpart of NGC 5128, Centaurus A, is no less peculiar. Early interferometric observations (Stanley and Slee 1950) indicated that it consists of two components: one, a strong source of small angular size coinciding in position with NGC 5128; the other, a broad, faint extended source surrounding NGC 5128. The extended source has been shown in good detail by recent pencil-beam observations at 19·7 Mc/s (Shain 1958) and at 85·5 Mc/s (Sheridan 1958). It is highly elongated in the north-south direction and covers an area of more than 20 square degrees. In the present paper we describe observations made to extend the picture to decimetre wavelengths. The results will be discussed in a later paper.

II. Instrumentation

The equipment used to make the observations described in the present paper consisted of units of the hydrogen-line receiver (at Potts Hill, near Sydney) used by Kerr, Hindman, and Gum (1959), modified to permit broadband detection of continuum radiation.

(a) *The Aerial*

The 36 ft transit-mounted paraboloidal reflector at Potts Hill was employed. The feed is a flanged horn attached to a four-legged support based on the rim of the reflector. Four separate calibrations were required to fix the aerial constants:

(i) *Calibration of the declination indicator*.—This has been described in detail by Kerr, Hindman, and Gum (1959). The declination setting is accurate to within $0°·05$.

(ii) *Determination of the instrumental meridian*.—Observations of discrete sources with well-determined positions show that the instrumental meridian does not deviate perceptibly from the true meridian.

(iii) *Measurement of the shape of the radiation pattern*.—This was done by observing the Sun and several discrete sources (Kerr, Hindman, and Gum 1959). The main lobe of the aerial pattern is circular, with a very nearly Gaussian cross section. The separation of the half-power points is $1°·4$. The first side lobes are 23 dB below the peak of the main lobe. Figure 1 shows a section of the beam, with a Gaussian curve for comparison.

(iv) *Measurement of the aperture efficiency*.—This was accomplished by comparing the gain of the aerial with the known gain of a sectoral horn, using the Sun as a transfer source. The peak gain of the paraboloid is $41·8 \pm 0·3$ dB, corresponding to an aperture efficiency of $0·56 \pm 0·04$.

When deriving the flux density of an extended object, one must know the gain of the aerial throughout a solid angle large enough to include the entire object for every beam position at which there is a measurable aerial temperature. In effect, this means that one must know how to convert observations of aerial temperature into a (smoothed) map of brightness temperature. The desired conversion factor, which we shall call the *net efficiency*, may be defined as that fraction of the total input power which would go into the main lobe if the aerial were used to transmit instead of to receive. In the case of the Potts Hill aerial, we have a net efficiency of 0·78 at 1400 Mc/s. It should be noted that the net efficiency must be multiplied by a factor depending on the angular extent of the source, if the source covers an appreciable fraction of 4π steradians.

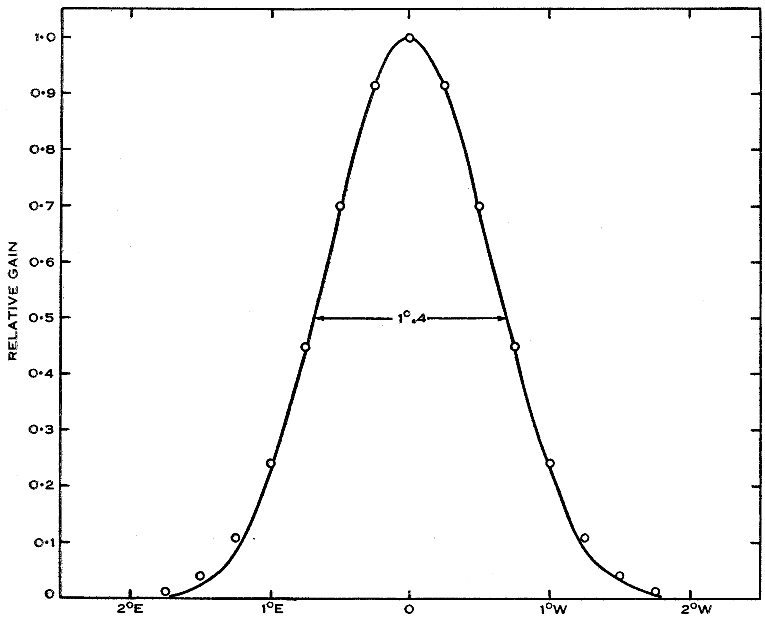

Fig. 1.—The measured shape of the main lobe of the radiation pattern of the 36 ft paraboloid at a frequency of 1400 Mc/s. The open circles indicate the form of a Gaussian curve with the same width between half-power points.

(*b*) *The Receiver*

Figure 2 is a block diagram of the receiving system. The i.f. bandwidth was approximately 2·7 Mc/s. No image rejection was used, so the system accepted noise from two bands each 30 Mc/s from the local oscillator frequency, 1393 Mc/s. Neither band included radiation from galactic neutral hydrogen. The receiver was a D.C. comparison radiometer which, in the present programme, measured the difference between the receiver output voltage and the voltage of a stable D.C. source. Long-term stability of the receiver was achieved by temperature control; the zero level remained constant to within about 2 °K for several hours at a time. No time constant other than that inherent in the pen recorder was used, because a short time constant facilitated the recognition of impulsive interference (mainly due to vehicles). The envelope of the noise fluctuations usually had a width of about 2 °K. The records could be read with an accuracy of about $\pm 0 \cdot 2$ °K; hence the short instrumental time constant had little influence on the attainable reading accuracy. The effective time constant introduced by averaging in the reduction process was about 30 sec.

The receiver calibration consisted of two steps. The first was a measurement of the receiver noise temperature with the aid of a discharge-tube noise generator. The measurement was made at the output of the second detector because of the limited range of the D.C. amplifier. The noise temperature of the receiver is given by

$$T_R = (1+\alpha)T_0 \frac{T_s/T_0 - P_1/P_0}{P_1/P_0 - 1}, \quad \ldots\ldots\ldots\ldots\ldots \quad (1)$$

where α=fraction of the image band accepted (=1 in our case),
T_0=ambient temperature,
T_s=effective temperature of the noise generator,
P_0=output power with the noise generator turned off, and
P_1=output power with the noise generator turned on.

T_0, T_s, and α are all known quantities. Hence the measurement required only a determination of P_1/P_0. During the period of observation, T_R was near 1800 °K.

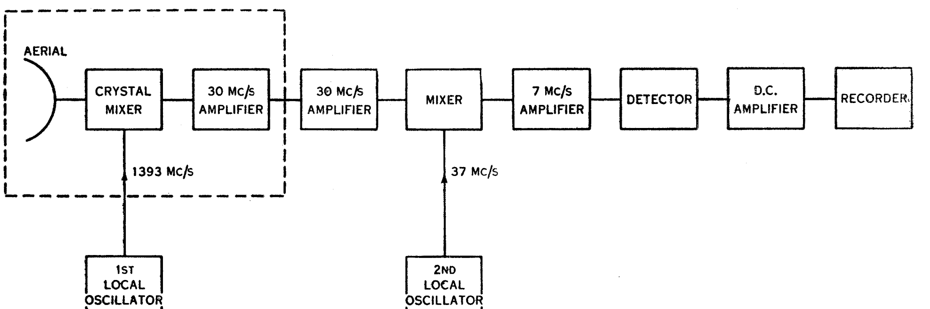

Fig. 2.—Block diagram of the receiving system.

The second step in the calibration was to relate a change in aerial temperature to the corresponding change in the deflection of the pen recorder. The fractional change in input power at the second detector corresponding to a small change ΔT_a in aerial temperature is

$$\frac{\Delta P}{P} = \frac{(1+\alpha)\Delta T_a}{T_R + (1+\alpha)T_a}. \quad \ldots\ldots\ldots\ldots\ldots\ldots \quad (2)$$

The detector of the Potts Hill radiometer is linear within the accuracy of our measurement. In the case of a linear detector, the fractional change in detector output voltage corresponding to $\Delta P/P$ is

$$\Delta V/V = \tfrac{1}{2}\Delta P/P. \quad \ldots\ldots\ldots\ldots\ldots\ldots\ldots\ldots (3)$$

Combining equations (2) and (3), we get

$$\Delta T_a = \frac{2T_R}{1+\alpha} \cdot \frac{\Delta V}{V}, \quad \ldots\ldots\ldots\ldots\ldots\ldots\ldots \quad (4)$$

provided $T_R \gg (1+\alpha)T_a$, which was true in the present series of measurements. Calibration of the D.C. amplifier gave the relation between $\Delta V/V$ and recorder deflection, from which one immediately obtains the increment in aerial temperature required to shift the recorder pen by one chart unit. During the present programme, the sensitivity was near $0 \cdot 5$ °K per chart division.

III. The Observations

The observations consist of drift curves made during meridian transit at intervals of $\frac{1}{2}$° in declination. Three to five observations were made on each declination, and from these a set of mean sections was derived. During many of the observations the aerial was directed towards the South Celestial Pole for 2 min every 10 or 15 min in order to obtain a fairly continuous check on the

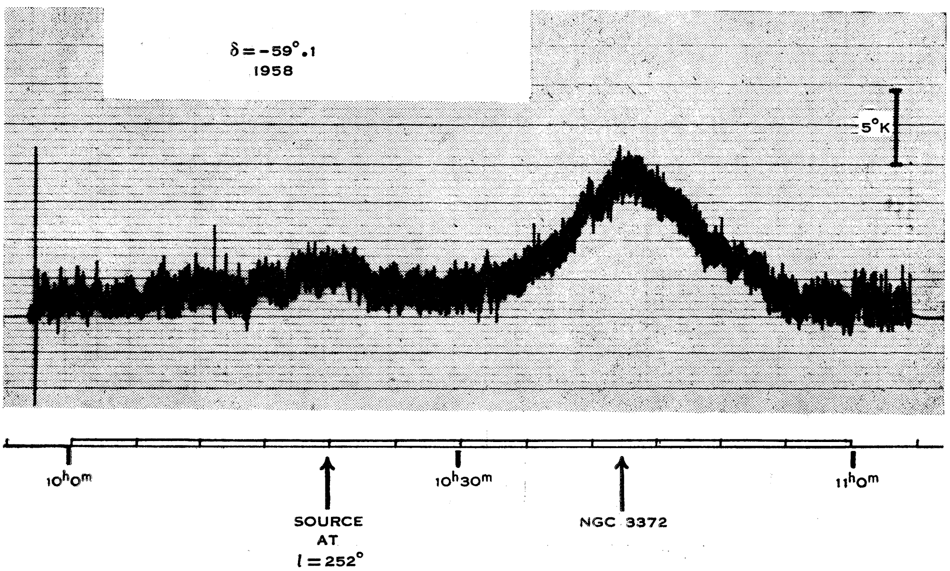

Fig. 3.—A constant-declination record taken at $\delta_{1958} = -59° \cdot 1$. This strip passes $0° \cdot 5$ north of NGC 3372 and $1° \cdot 5$ south of the source at $l=252°$. Right Ascensions for the epoch $1958 \cdot 0$ are indicated. The sensitivity is $0 \cdot 55$ °K per small chart division.

zero-level stability of the receiver over the period of the observation. The zero level adopted for the reduction of each observation was that corresponding to the south pole. The actual zero level, however, depended on the declination setting of the aerial because the amount of radiation received from the ground through the side and back lobes of the aerial pattern varied with the altitude towards which the main lobe was directed. Therefore the variation of receiver output level as a function of declination had to be determined separately in order that all the mean sections could be referred to a common zero level. While the corrections were all small, some were large enough to be significant; the largest amounted to 2 °K. A further check on the calibration of the zero levels was obtained by scanning the regions in declination several times during transits. A selected record is shown in Figure 3.

(a) *The Eta Carinae Region*

The contour diagram of the Eta Carinae region (Fig. 4) was drawn from the mean sections. The outer contour, marked 0 °K, delineates the boundary of detectable radiation. The quantity shown is aerial temperature as a function of position (in galactic coordinates, referred to Ohlsson's pole). The distribution of brightness temperature (as smoothed by the aerial beam) may be found by dividing the aerial temperatures by the net efficiency factor for the aerial. The source at $l=255°$ is NGC 3372 ; the other source, at $l=252°$, is not related to any object known optically, but it was recorded in the survey by Hill, Slee, and Mills (1958) at 3·5 m wavelength. It is evident that an appreciable amount of radiation from the galactic disk is present on the high longitude side of NGC 3372, with the maximum intensity of the ridge occurring at $b\approx -0°\cdot 8$.

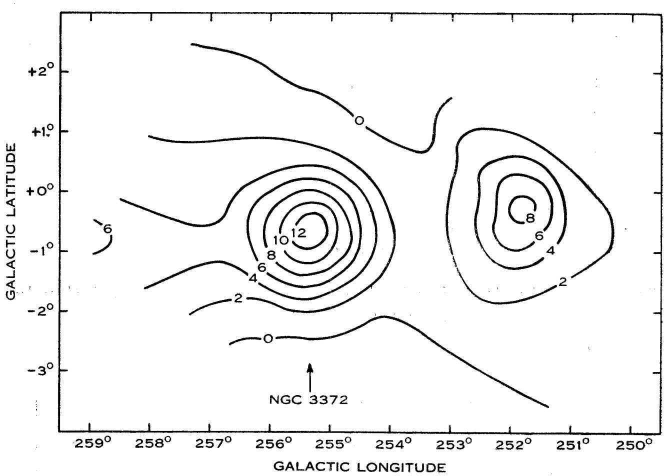

Fig. 4.—Map of aerial temperature as a function of position in the vicinity of NGC 3372. The contour interval is 2 °K. The contours marked 0 °K show the limits of detectable radiation. The coordinates are based on Ohlsson's galactic pole, $\alpha_{1900}=12^{\mathrm{h}}\ 40^{\mathrm{m}}$, $\delta_{1900}=+28°$.

Before deriving the flux density of NGC 3372, it was necessary to subtract the radiation due to the galactic disk. This was accomplished by a linear interpolation between constant longitude sections outside the nebula on either side, at $l=253°\cdot 5$ and at $l=257°\cdot 5$. The resulting form for the estimated distribution of the disk radiation is shown in Figure 5. Subtraction of this from the observed distribution yields the source brightness distribution shown in Figure 6. The maximum net aerial temperature, 10 °K, occurs at $l=255°\cdot 3$, $b=-0°\cdot 6$. Table 1 shows the agreement between this position and previous radio and optical determinations. The small discrepancy between the two optically determined positions is due to the difficulty in defining accurately the centre of an extended and somewhat irregular object.

Integration of the contours shown in Figure 6 leads to a value of $5\cdot 82\times 10^{-24}$ W m^{-2} (c/s)$^{-1}$ for the flux density of NGC 3372 near 1400 Mc/s.

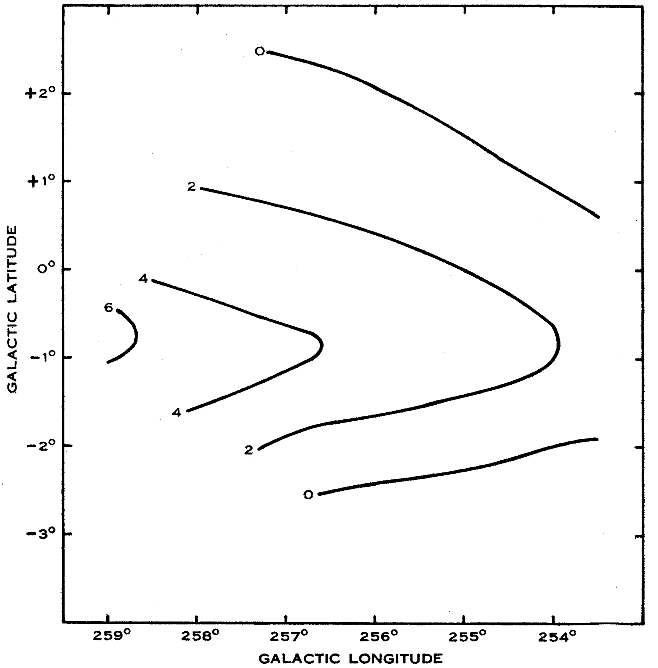

Fig. 5.—Estimated distribution of the galactic disk radiation in the vicinity of NGC 3372.

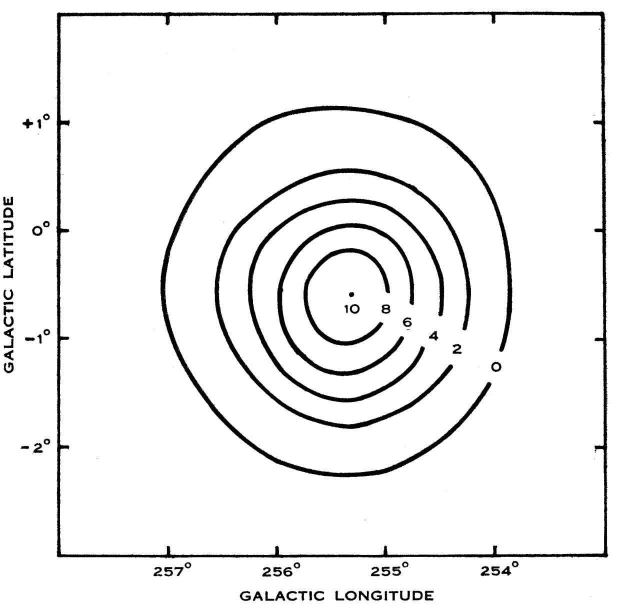

Fig. 6.—Contours of NGC 3372 after subtraction of the galactic disk radiation.

The accuracy of this figure is not easy to estimate, since several sources of uncertainty must be considered. These are:

(i) *Aerial calibration.*—The relevant quantity is the net efficiency, which depends on the aerial gain and the form of the radiation pattern. The latter is known quite accurately, but the gain is less well determined. We estimate that the maximum error in the net efficiency is about ± 10 per cent.

(ii) *Receiver calibration.*—This measurement is straightforward and should be accurate to within ± 10 per cent.

(iii) *Errors in the mean sections and in the subtraction of the galactic disk radiation.*—The mean sections are subject to some uncertainty because of the thermal noise fluctuations in the receiver output and residual errors in the adopted zero levels. While the procedure used to subtract the galactic disk radiation was impersonal, it certainly was not perfectly accurate. The estimated maximum error from these causes is ± 10 per cent.

The uncertainty due to the above causes probably is under ± 20 per cent. The greatest error, which would apply if all of the above uncertainties were additive, does not exceed ± 30 per cent.

The flux density of the source at $l=252°$ is 5×10^{-24} W m^{-2} (c/s)$^{-1}$. This result is only approximate, since our observations do not cover an area large enough to permit a good estimate of the galactic background level under the source.

TABLE 1

COMPARISON OF RADIO AND OPTICAL POSITIONS FOR NGC 3372

Frequency	l	b	Estimated Maximum Error	Reference
1400 Mc/s	255°·3	—0°·6	±0°·1	Present paper
85·5 Mc/s	255°·4	—0°·7	±0°·1	Hill, Slee, and Mills (1958)
Optical	255°·3	—0°·5	—	Cederblad (1946)
Optical	255°·2	—0°·8	—	Gum (1955)

(*b*) *Centaurus A*

The observed distribution of 1400 Mc/s radiation from Centaurus A is shown in Figure 7. The limit of detectable radiation is indicated by the contour marked "0". The object lies nearly 20° from the galactic plane, and there is no detectable galactic continuum emission in its vicinity. The region north of $\delta=-41°$ is too faint to be well observed with our equipment, so the contours in that region are shown as dashed lines. The source evidently comprises two distinct components:

(i) A primary maximum at $\alpha_{1950}=13^{\mathrm{h}}\,22^{\mathrm{m}}\cdot 9$, $\delta_{1950}=-42°\,45'$, which seems almost certainly to be associated with the peculiar galaxy NGC 5128.

(ii) A very extensive source covering some 20 square degrees, which probably is associated physically with the primary source. There is a strong, broad maximum in the intensity of this component at $\alpha_{1950} \approx 13^h\ 20^m \cdot 5$, $\delta_{1950} \approx -44^\circ \cdot 7$. Two weak secondary maxima are suspected in the northern part of the object, at $\alpha_{1950} \approx 13^h\ 20^m$, $\delta_{1950} \approx -40^\circ \cdot 3$ and at $\alpha_{1950} \approx 13^h\ 24^m$, $\delta_{1950} \approx -39^\circ \cdot 1$.

On the whole, Figure 7 bears a remarkably close resemblance to the 85·5 Mc/s chart published by Sheridan (1958).

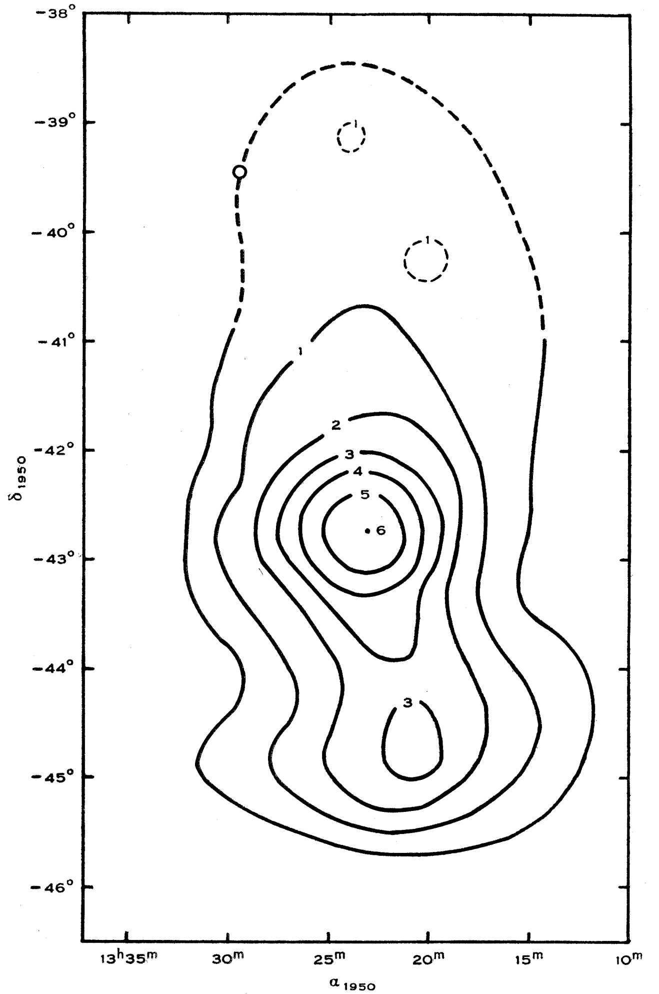

Fig. 7.—Map of aerial temperature for Centaurus A as a function of position in equatorial coordinates (epoch 1950).

The position found for the primary maximum is in satisfactory agreement with the results obtained previously at metre wavelengths, as shown in Table 2. The slightly higher value for the Right Ascension determined at 1400 Mc/s may be due partly to the skewness of the primary source, observed by Sheridan

TABLE 2

POSITION MEASUREMENTS FOR CENTAURUS A

Frequency	α_{1950}	δ_{1950}	Reference
1400 Mc/s	$13^h\ 22^m{\cdot}9 \pm 0^m{\cdot}5$	$-42°\ 45' \pm 6'$	Present paper
100 Mc/s	$13^h\ 22^m{\cdot}5 \pm 0^m{\cdot}07$	$-42°\ 46' \pm 2'$	Mills (1952)
85·5 Mc/s	$13^h\ 22^m{\cdot}4 \pm 0^m{\cdot}2$	$-42°\ 41' \pm 4'$	Sheridan (1958)
Optical (NGC 5128)	$13^h\ 22^m{\cdot}4$	$-42°\ 45'$	de Vaucouleurs (1956)

with a beamwidth of 50′. The skewness is such that the primary source profile is less steep on the eastern side, hence the greater beamwidth of our aerial (nearly twice that used by Sheridan) probably results in a slight shift of the observed maximum intensity towards a higher Right Ascension at 1400 Mc/s.

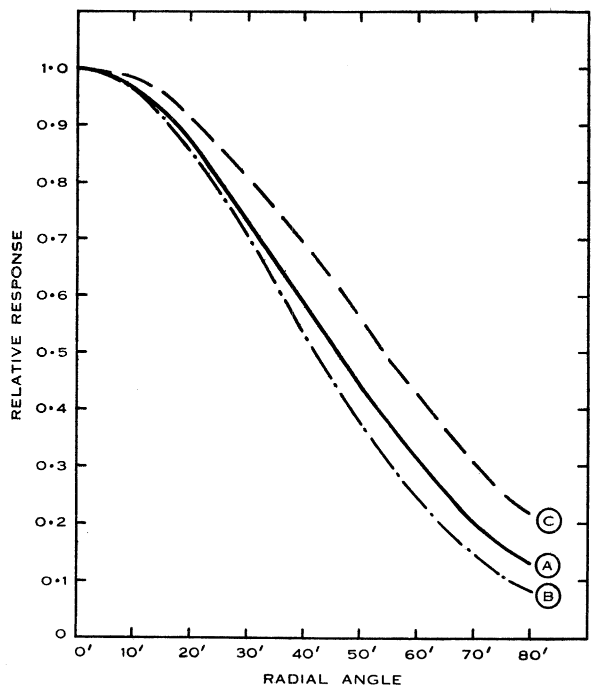

Fig. 8.—Apparent radial brightness distributions : *A*, observed mean for NGC 3372 ; *B*, point source smoothed by the aerial beam ; *C*, uniform optically thin sphere 2°·0 in diameter smoothed by the aerial beam.

The integrated flux density of the entire object is $1{\cdot}3 \times 10^{-23}$ W m^{-2} (c/s)$^{-1}$ at 1400 Mc/s, with an estimated probable error of ± 20 per cent. Of this about 3×10^{-24} W m^{-2} (c/s)$^{-1}$, or 23 per cent., arises in the primary source; the remainder is due to the extended component.

IV. Conclusions

(a) *The Eta Carinae Nebula*

Figure 6 suggests that NGC 3372 possesses a high degree of radial symmetry in its overall surface brightness distribution. This is implied by the circularity of the contours and by the central location of the maximum observed brightness. Small-scale irregularities, if present, cannot be seen because the aerial beam has a size of the same order as that of the object. Nevertheless, any strong large-scale asymmetry would result in a noticeable distortion of the contours.

The true surface brightness distribution across NGC 3372 cannot be derived from the observed distribution (Bracewell and Roberts 1954). It is possible, however, to judge whether the source shows an appreciable central condensation. Curve A in Figure 8 is the observed mean radial brightness distribution. Curve B is the expected response to a point source (see Fig. 1). Curve C is the computed response to a uniform optically thin sphere (semi-elliptical true radial surface brightness distribution) with the same angular diameter as NGC 3372 ($2^\circ \cdot 0$). Comparison of curves A and B indicates that the source must have an appreciable angular width, while comparison of curves A and C implies that it must be strongly concentrated towards its centre. This conclusion is in agreement with unpublished measurements in Hα light made by C. S. Gum, which show that the object has an intense central core about $24'$ in diameter, and that the surface brightness in the outer regions is much lower.

The observational results may be summarized as follows:

(i) The flux density of NGC 3372 near 1400 Mc/s is $5 \cdot 82 \times 10^{-24}$ W m^{-2} (c/s)$^{-1}$, with an estimated probable error less than ± 20 per cent.

(ii) There is no marked large-scale asymmetry in its surface brightness distribution.

(iii) The source is strongly concentrated towards its centre.

The results will be discussed in a second paper (Wade 1959).

(b) *Centaurus A*

We have found that the appearance of Centaurus A (13S4A) at 1400 Mc/s is similar to that previously observed at $85 \cdot 5$ Mc/s by Sheridan (1958). The source consists of two components: one is a point source evidently associated with the peculiar galaxy NGC 5128; the other is a very large extended source with no known optical counterpart. A striking feature is the strong maximum in the intensity of the extended source, about 2° south of the point source. The total flux density at 1400 Mc/s is $1 \cdot 3 \times 10^{-23}$ W m^{-2} (c/s)$^{-1}$, with an estimated probable error of ± 20 per cent. Of this, about 23 per cent. arises in the point source, and 77 per cent. comes from the extended source.

The results will be discussed in a subsequent paper.

V. Acknowledgment

One of us (C.M.W.) is indebted to the Commonwealth Scientific and Industrial Research Organization for a Junior Research Fellowship.

VI. References

Bailey, S. I. (1908).—*Ann. Harv. Coll. Obs.* **60** : 199.
Bok, B. J. (1932).—Harv. Repr. No. 77.
Bok, B. J., Bester, M. J., and Wade, C. M. (1955).—*Proc. Amer. Acad. Arts Sci.* **86** : 9.
Bolton, J. G., Stanley, G. J., and Slee, O. B. (1949).—*Nature* **164** : 101.
Bracewell, R. N., and Roberts, J. A. (1954).—*Aust. J. Phys.* **7** : 615.
Cederblad, S. (1946).—Medd. Lunds Astr. Obs. (II) No. 119.
Gum, C. S. (1955).—*Mem. R. Astr. Soc.* **67** : 155.
Hill, E. R., Slee, O. B., and Mills, B. Y. (1958).—*Aust. J. Phys.* **11** : 530.
Kerr, F. J., Hindman, J. V., and Gum, C. S. (1959).—*Aust. J. Phys.* **12** : 270.
Mills, B. Y. (1952).—*Aust. J. Sci. Res.* A **5** : 456.
Mills, B. Y., Little, A. G., and Sheridan, K. V. (1956).—*Aust. J. Phys.* **9** : 218.
Shain, C. A. (1958).—*Aust. J. Phys.* **11** : 517.
Sheridan, K. V. (1958).—*Aust. J. Phys.* **11** : 400.
Stanley, G. J., and Slee, O. B. (1950).—*Aust. J. Sci. Res.* A **3** : 234.
de Vaucouleurs, G. (1956).—Mem. Commonw. Obs. Aust. No. 13.
Wade, C. M. (1959).—*Aust. J. Phys.* **12** (4). (In press.)
Westerhout, G. (1958).—*Bull. Astr. Insts. Netherlds.* **14** : 215.